International Journal of Applied Engineering Research ISSN 0973-4562 Volume 14, Number 18 (2019) pp. 3708-3712

Study on performance of High Altitude Platform Systems over a shadowed Rician fading channel

Hien Thi Thu Nguyen
Faculty of Telecommunications 1, Posts and Telecommunications Institute of Technology, Km10, Nguyen Trai Street, Ha Dong District, Hanoi, Vietnam.

Abstract

In this paper, we present the research results on design and evaluating performance of channel codes used in High Altitude Platform (HAP) systems over a shadowed Rician fading channel. The shadowed Rician channel is a generalization of the Rician model, where the amplitude of the line-of-sight component is subjected to the complete or partial blockage by buildings, trees, hills, mountains, etc., and is characterized by the Nakagami distribution. To achieve better performance, we use and design a Irregular Convolutional Code (IrCC) to approach the Discrete-input Continuous-output Memoryless Channel (DCMC) capacity with a given code rate and modulation method. Therefore, DCMC capacity for HAP systems over a shadowed Rician fading channel must be calculated. These capacity curves establish an upper bound that performance of HAP systems using channel codes is expected to reach. Furthermore, we also evaluate performance on Bit Error Rate (BER) of the HAP system using the designed channel codes.

Keywords: High Altitude Platform, Shadowed Rician Fading Channel, DCMC, Exit Chart, Irregular Convolutional Code.

INTRODUCTION

High Altitude Platform (HAP) broadband communication is expected to become a popular solution for the wireless communications infrastructure [1]. HAP networks have been increasingly playing an important role in supporting broadband wireless communication systems, namely fourth generation Long Term Evolution (4G-LTE) and fifth generation (5G) networks [2]. HAPs are communication facilities situated at an altitude of 17 to 30 km and at a particular point relative to the Earth. The significance of such systems is rapidly growing for a variety of applications such as broadband wireless access, navigation and positioning systems, remote sensing and weather observation/monitoring systems, mobile telephony as well as digital TV [3].

The quality of service provided by HAP systems strongly depends on the propagation channel between HAP and the land user. During propagation, the wireless signal is normally influenced by path loss, shadows, and multipath fading. In the HAPs communication scenario, it is generally believed that the Rician fading characteristic is appropriate, which includes the line-of-sight (LOS) and non-LOS (NLOS) components [4]. However, the LOS component is frequently shadowed by trees, buildings, and other obstacles, therefore if we further take the shadows into consideration [5].

Following the research results of the serially concatenated coding schemes for HAP system in CAPANINA project [6], we use an Irregular Convolutional Code (IrCC) [7,8] in outer encoder by to improve near-capacity performance for HAP systems under shadowed LOS condition. Our approach is based on invoking Extrinsic Information Transfer (EXIT) chart analysis [9] - a powerful semi-analytical tool, to design near-capacity channel codes.

Against this background, the novel contribution of this paper is that we compute the DCMC capacity of HAP systems over a shadowed Rician fading channel and present the design & performance results of near-capacity channel codes for HAP system over this channel model. The rest of the paper is organized as follows. In Section 2, a review of the HAP propagation channel model and computing the DCMC channel capacity is considered. In Section 3, the research results of channel code design and performance of HAP systems over a shadowed Rician fading channel is represented. Finally, conclusion is offered in Section 4.

CHANNEL MODEL AND DCMC CAPATITY FOR HAP

The quality of service provided by HAP systems strongly depends on the propagation channel between the HAP and the land user. As such, an accurate statistical model for the HAP channel is required for calculating fade margins, assessing the average performance of modulation and coding schemes, analyzing the efficiency of communication protocols, and so on. The random fluctuations of the signal envelope in a narrowband HAP channel can be attributed to two types of fading: multipath fading and shadow fading [10]. We further divide the shadow fading into the line-of-sight (LOS) shadow fading and multiplicative shadow fading. Notice that the multipath components consist of a LOS component and many weak scatter components.

In an ideal HAP channel without any type of fading, where there is a clear LOS between the HAP and the land user, without any obstacle in between, hence, no scatter component, the envelope is a non-random constant. Due to multipath fading, caused by the weak scatter components propagated via different non-LOS (NLOS) paths, together with the non-blocked LOS component, the envelope becomes a Rice random variable. LOS shadow fading comes from the complete or partial blockage of the LOS by buildings, trees, hills, mountains, etc., which in turn makes the amplitude of the LOS component a random variable. On the other hand, multiplicative shadow fading refers to the random variations of the total power of the multipath components, both the LOS and NLOS components.

In this paper, the shadowed Rician fading channel model considered is a Rician fading channel model in which the LOS component is random. Due to the power of the LOS component is assumed to be a gamma random variable. Since the square root of a gamma variable has Nakagami distribution [11], this means that amplitude of the LOS component is modeled with a Nakagami distribution [12].This approach offers significant analytical and numerical advantages for system performance evaluation, design issues, etc.

Assume that the lowpass-equivalent complex envelope of the stationary narrowband shadowed Rice single model can be written as

$$\Re(t) = A(t)\exp\left[j\alpha(t)\right] + Z(t)\exp\left[j\zeta_0\right] \qquad (1)$$

where $\alpha(t)$ is the stationary random phase process with uniform distribution over [0,2π), while ζ_0 is the deterministic phase of the LOS component. The independent stationary random processes *A(t)* and *Z(t)*, which are also independent of $\alpha(t)$, are the amplitudes of the NLOS and the LOS components, following Rayleigh and Nakagami distributions, respectively

$$p_A(a) = \frac{a}{b_0}\exp\left(\frac{-a^2}{2b_0}\right), \quad a \geq 0,$$
$$p_Z(z) = \frac{2m^m}{\Gamma(m)\ \Omega^m} z^{2m-1}\exp\left(\frac{-m z^2}{\Omega}\right), \quad z \geq 0, \qquad (2)$$

where $2b_0$ is the average power of the scatter component, Γ(.) is the gamma function, *m* is the Nakagami parameter, and Ω is the average power of the LOS component.

Let us define the envelope as $R(t) = |\Re(t)|$. The shadowed Rician PDF for the signal envelope can be written as [12]

$$p_R(r) = \left(\frac{2b_0 m}{2b_0 m + \Omega}\right)^m \frac{r}{b_0}\exp\left(-\frac{r^2}{2b_0}\right) {}_1F_1\left(m, 1, \frac{\Omega r^2}{2b_0(2b_0 m + \Omega)}\right), \ r \geq 0 \qquad (3)$$

where ${}_1F_1$ is the confluent hypergeometric function [28].

The shadowed Rician PDF and CDF are approximated according to a set of parameters (b_0, Ω, *m*) and showed in Figure 1. The relationship between the two sets of parameters (Ω, *m*) in (3) and (δ, μ) [5] in Lognormal distribution can be established [12]

$$\mu = \frac{1}{2}\left|\ln\left(\frac{\Omega}{m}\right) + \Psi(m)\right|,$$
$$\delta^2 = \frac{\Psi'(m)}{4}, \qquad (4)$$

where $\Psi(.)$ and $\Psi'(.)$ are the psi function and its derivative, respectively [28]. These parameters are computed according to $b_0 = \frac{\Omega}{2.10^{K[dB]/10}}$, $\mu = \frac{\ln 10}{20}\mu[dB]$, $\delta = \frac{\ln 10}{20}\delta[dB]$, formulas (4) and are listed in Table 1.

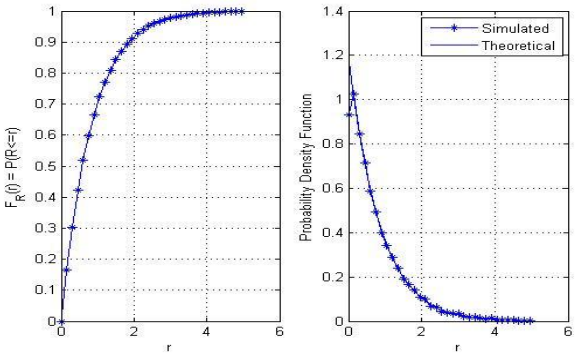

Figure 1: An approximated Shadowed Rician CDF and PDF of light shadowing with Rician factor K = 10 dB

Table 1: List of two sets of parameters (Ω, m) in (4) and (δ, μ) [5] over a a shadowed Rician fading channel (Rician fator *K*=10 dB)

Severity of the shadowing	Parameters of Lognormal PDF in []		Parameters of shadowed Rician PDF for HAP system		
	μ	δ	b_0	*m*	Ω
Light shadowing	0.115	0.173	0.4896	8.8	1.33
Heavy shadowing	-3.9	0.806	$0.46\text{x}10^{-4}$	0.74	$9.2\text{x}10^{-4}$
Average shadowing	-0.119	0.403	0.4063	1.99	1.03

Let's consider a wireless communication scenario between an HAP and the mobile user. The binary data stream is first modulated and mapped to a sequence of complex modulation symbols. The modulated sequence x is transmitted over the wireless channel and the sequence y is received in the receiver. The received signal can be represented as

$$y = hx + n \qquad (5)$$

where *h* is the shadowed Rician fading coefficient that fluctuates on a symbol-by-symbol basis, and *n* is the AWGN process having a variance of $N_0/2$ per dimension.

The theoretical DCMC capacity is described in [13] and is calculated by formula (1) in [14] as follows

$$C_{(\eta)}^{DCMC}(R) = \eta - \frac{1}{M}\sum_{l=1}^{M} E\left[\log_2 \sum_{z=1}^{M}\exp\left(\psi_{l,z}\right)\Big|_{X_l}\right] \text{[BPS]}, \qquad (6)$$

where $M = 2^\eta$ is the number of modulation levels, while η is the number of modulated bits and $E[A \mid X_l]$ is the expectation of *A* conditioned on the *M*-ary signals X_l. It is worth to note that $\psi_{l,z}$ is a function of both the transmitted

signal and of the channel as defined in [18]. For the system relying on a single transmit and a single receiver antenna, we have

$$\psi_{l,z} = \frac{-\left|h\left(x_l - x_z\right) + n\right|^2 + \left|n\right|^2}{N_0} \tag{7}$$

where *h, x* and *n* are the shadowed Rician the fading coefficient, the transmitted signal and the AWGN, respectively.

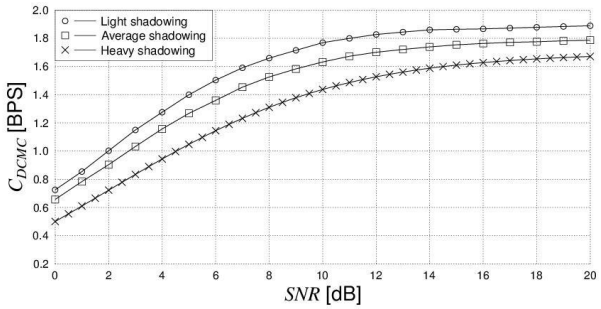

Figure 2: DCMC capacity for HAP system using QPSK over a shadowed Rician fading channel (Rician fator K=10 dB).

By employing the classic Monte Carlo simulation method for averaging the expectation terms. The capacity curves of the DCMC with different shadowing levels over shadowed Rician fading channels, when employing Quadrature Phase Shift Keying (QPSK) are shown in Fig.2. Evidently, at a given information rate *R*, we can completely identify the corresponding receiver's faded signal to noise power ratio $SNR_r\big|_R$. Similarly, DCMC capacity of a shadowed Rician fading channel when using other modulation methods such as 8 level Phase Shift Keying (8PSK), 16 level Quadrature Amplitude Modulation (16QAM) can also be calculated. Therefore, depending on the condition of the channel, suitable modulation schemes can be adjusted to achieve the desired capacity.

THE RESULTS OF CHANNEL CODE DESIGN AND PERFORMANCE OF HAP SYSTEM OVER A SHADOWED RICIAN FADING CHANNEL

It should be noted that the capacity of an inner arrangement sets an upper bound for the capacity of an outer arrangement [19]. Hence, according to the afore-listed order, the capacity associated with the inner most arrangement DCMC-QPSK sets the maximum achievable capacity for all systems employing the other schemes.

In this section, we design near-capacity channel codes for HAP system by using IrCC in the outer encoder of an serial concatenation convolutional code (SCCC) coding scheme in CAPANINA project [6] (Fig.3). For the inner coder, a Unity-Rate Code (URC) is used as a precoder for creating an Infinite Impulse Response (IIR) inner demapper component in order to reach the (1,1) EXIT chart convergence point and hence to achieve an infinitesimally low BER.

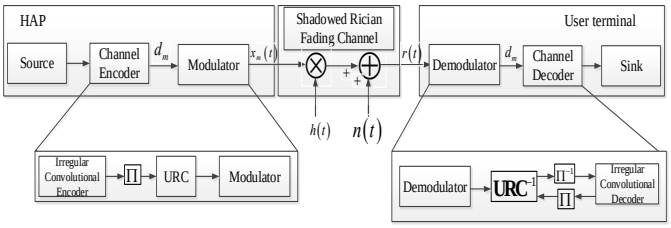

Figure 3: IrCC-URC-MOD Coding Scheme for HAP system.

For the IrCC, we use IrCC having 8 subcodes with code rates R_k from 0.2 to 0.9. These subcodes are created from memory-3 mother code defined by generators (17, 15) that has code rate R_c =0.5. If $R_k<R_c$, two generators (13, 11) is added and punctured, also if $R_k>R_c$, only puncturing is performed. Therefore, each subcode encodes a fraction of $\alpha_k r_k L$ information bit to $\alpha_k L$ code bits, where α_k, r_k is weight and code rate of k^{th} subcode, *L* is number of information bits.

We denote these subcodes with the tuples $\{R_k, [w_0, w_1, ...], l_i, [p_0, p_1, ...]\}$, where $k = 1,2,...8$, w_j, $j = 0,1,2,3$ denotes the frequency of occurrence of g_j in the generator matrix, l_i is the puncturing period and p_j is the puncturing pattern associated to g_j (in octal) as follow [8]:

$\{0.2,(1,2,1,1),1,(1,1,1,1)\}$, $\{0.3,(1,1,1,1),3,(7,7,7,1)\}$,
$\{0.4,(1,1,1),2,(3,3,1)\}$, $\{0.5,(1,1),1,(1,1)\}$, $\{0.6,(1,1),3,(7,3)\}$,
$\{0.7,(1,1),7,(177,025)\}$, $\{0.8,(1,1),4,(17,1)\}$,
$\{0.9,(1,1),9,(777,1)\}$.

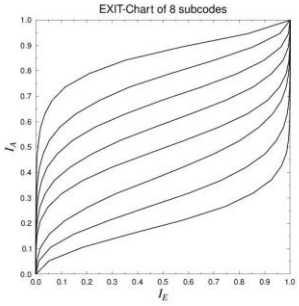

Figure 4: EXIT chart of 8 subcodes from mother code CC(17,15).

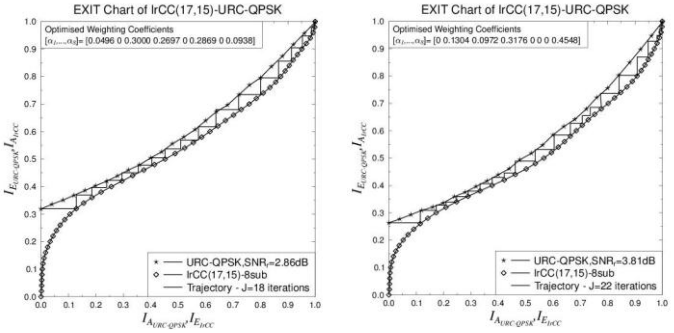

(a) (b)

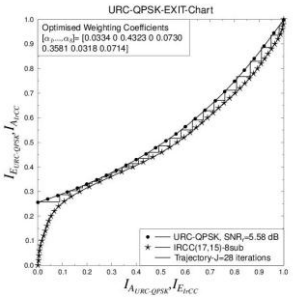

(c)

Figure 5: EXIT chart for IrCC(17,15)-URC-QPSK over a shadowed Rician fading channel (Rician fator K=10 dB): (a) Light shadowing, (b) Average shadowing, (c) Heavy shadowing.

Results of EXIT curves for 8 subcodes are shown in Fig.4. Based on these EXIT curves, the task of fitting outer coder's transfer function with given code rate to a given inner coder's transfer function while satisfying (8) in [13]. As a result, we obtain the EXIT curves of IrCC-URC-QPSK coding scheme and the corresponding optimized weighting coefficients α_k, k=1,...,8 for the IrCC(17,15) coder R_c=0.5, with the Monte-Carlo simulation based decoding trajectory, as shown in Fig. 5.

For example, with code rate R_c=0.5, we use 5 subcodes with code rates 0.2, 0.4, 0.5, 0.7 and 0.9. Furthermore, we also determine weighting coefficients of 8-subcode IrCC(17,15) $[\alpha_1, \alpha_2, ..., \alpha_8]$=[0.0496 0 0.3 0.2697 0 0.2869 0 0.0938]. It means that each subcode encodes a fraction of 496/3000/2697/2869/938 input information bit of frame lengh 10000 bits.

BER performance of these coding schemes is also presented in Fig. 6. These simulation results supports the accuracy of EXIT chart analysis presented in Fig. 5.

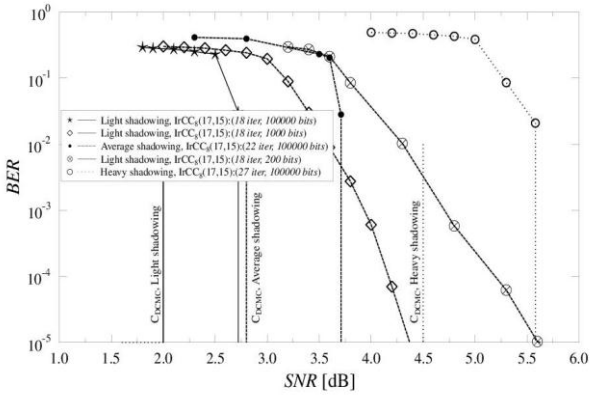

Figure 6: Performance BER of $IrCC_8$(17,15)-URC-QPSK coding scheme for HAP system over a shadowed Rician fading channel, code rate R_c=0.5.

Obviously, the value of the 'turbo-cliff' SNR given in Fig. 6 with the number of iterations needed to converge to the point (1,1) indicates that as we inferred from EXIT-chart analysis. Once the SNR value exceeds this value, the BER of the coding scheme is expected to become infinitesimally low. Furthermore, with code rate R_c=0.5, IrCC(17,15)-URC-QPSK's coding is far away from the DCMC capacity about 0.86/1.01/1.08 dB with frame size 100000 bits and 18/22/28 iterations corresponding to light shadowing, average shadowing and heavy shadowing. These gaps can be reduced when using IrCC with more components (>8), or using mother code with greater constraint length. However, the complexity of the number of decoding iterations also increases. Furthermore, if the frame length or number of decoding iterations is reduced, the performance BER degrades (Fig. 6).

CONCLUSIONS

In this paper, we presented the computing results of DCMC capacity for HAP systems over shadowed Rician fading channel. We have also designed a 8-subcode IrCC(17,15) and evaluated performance of these codes with code rates R_c=0.5 for HAP systems using QPSK modulation scheme. Obviously, using IrCC in HAP system achieves better performance (lower BER) and and approaches closer to DCMC. However, the complexity of the number of decoding iterations also increases. These above research results will be the basis for design and deployment of HAP systems in communications industry.

ACKNOWLEDGEMENT

The authors would like to thank to Motorola Solutions Foundation for supporting this research.

REFERENCES

[1]. F. Dong, Y. He, X. Zhou, Q. Yao, and L. Liu, "Optimization and design of HAPs broadband communication networks," in 2015 5th International *Conference on Information Science and Technology* (ICIST), pp. 154–159, IEEE, 2015.

[2]. D. Grace and M. Mohorcic, Broadband Communications via High Altitude Platforms. John Wiley & Sons, 2011.

[3]. F. A. Oliveira, F. C. L. d. Melo, and T. C. Devezas, "High altitude platforms present situation and technology trends," *Journal of Aerospace Technology and Management*, vol. 8, no. 3, pp. 249–262, 2016.

[4]. Liu, Yiming, David Grace, and Paul D. Mitchell. "Exploiting platform diversity for GoS improvement for users with different High Altitude Platform availability." *IEEE Transactions on Wireless Communications* 8.1 (2009): 196-203

[5]. Dong, Feihong, et al. "Diversity performance analysis on multiple HAP networks." *Sensors* 15.7 (2015): 15398-15418.

[6]. A. Boch, M. Laddomada, M. Mondin, and F. Daneshgaran, "Advanced channel coding for hap-based broadband services [internetworking and resource

management in satellite systems series],” *IEEE Aerospace and Electronic Systems Magazine*, vol. 22, no. 9, pp. C–7, 2007.

[7]. M. Tüchler, “Design of serially concatenated systems depending on the block length," *IEEE Trans. Commun*., vol. 52, no. 2, pp. 209-218, Feb. 2004.

[8]. M. Tuchler and J. Hagenauer, “Exit charts of irregular codes,” 2002

[9]. S. Ten Brink, “Designing iterative decoding schemes with the extrinsic information transfer chart,” AEU Int. J. Electron. Commun, vol. 54, no. 6, pp. 389–398, 2000.

[10]. B. Vucetic, “Propagation,” in *Satellite Communications-Mobile and Fixed Services*. M. J. Miller, B. Vucetic, and L.Berry, Eds., Boston, MA: Kluwer, 1993, pp. 57-101.

[11]. G. L. Stuber, Principles of Mobile Communication. Boston, MA: Kluwer, 1996.

[12]. Abdi, Ali, et al. "A new simple model for land mobile satellite channels: first-and second-order statistics." *IEEE Transactions on Wireless Communications* 2.3 (2003): 519-528.

[13]. L. Hanzo, C. H. Wong, and M. S. Yee, Adaptive Wireless Transceivers: TurboCoded, TurboEqualized and Space Time Coded TDMA, CDMA, and OFDM Systems. Chichester, UK: John Wiley IEEE Press, August 2002.

[14]. S. Ng and L. Hanzo, “On the mimo channel capacity of multi-dimensional signal sets,” in *Vehicular Technology Conference*, 2004. VTC2004-Fall. 2004 IEEE 60th, vol. 3, pp. 1594–1598, IEEE, 2004.

[15]. Tang, Chaoqing, Hequn Liu, and Gaofeng Pan. "Performance analysis of log-normal and Rayleigh-lognormal fading channels." 2014 12th *International Conference on Signal Processing* (ICSP). IEEE, 2014.